J Appl Electrochem (2008) 38:793–802
DOI 10.1007/s10800-008-9512-8

ORIGINAL PAPER

Influence of the Teflon loading in the gas diffusion layer of PBI-based PEM fuel cells

J. Lobato · P. Cañizares · M. A. Rodrigo · C. Ruiz-López · J. J. Linares

Received: 9 October 2007 / Revised: 4 February 2008 / Accepted: 4 February 2008 / Published online: 21 February 2008

Abstract The influence of the PTFE content in commercial Toray graphite paper gas diffusion layer (GDL) on the performance of a PBI-based polymer electrolyte membrane fuel cell (PEMFC) has been studied. These materials have been characterised by evaluating the porosity, pore size distribution, SEM micrographs, hydrophobicity, air permeability and electrical resistance. Fuel cell results show that the lower the Teflon content, the better the cell performance and the lower the losses when oxygen was replaced by air. These results led to non-Teflonized carbon paper to be postulated as the most suitable candidate, provided that its mechanical integrity can be maintained throughout the whole process of preparation and testing of the MEA. However, some practical problems with this type of commercial non-Teflonized carbon paper were experienced in this work and led to damage of the support. The detrimental effects are described and discussed. As conclusion, the use of a minimally PTFE-loaded (10%) carbon paper is suggested because the inclusion of this level of Teflon improved properly the mechanical properties of the carbon support and only caused a very small drop in the performance.

Keywords High temperature PEMFC · Polybenzimidazole · Gas diffusion layer · Teflon loading · Cell performance

J. Lobato (✉) · P. Cañizares · M. A. Rodrigo · C. Ruiz-López · J. J. Linares
Chemical Engineering Department, University of Castilla-La Mancha, Avda. Camilo José Cela s/n, 13004 Ciudad Real, Spain
e-mail: justo.lobato@uclm.es

1 Introduction

Polymer electrolyte membrane fuel cells (PEMFCs) are widely based on the use of perfluorinated materials (Nafion® and similar) as electrolytic membranes. Some of the qualities of these materials are high ionic conductivity when fully hydrated (≈ 0.1 S cm^{-1}), excellent mechanical strength and a demonstrated reliability during operation for more than 50,000 h [1]. However, Nafion® membranes need to be hydrated in order to be proton conductors, thus limiting the operational temperature to 90 °C at atmospheric pressure. This leads to some disadvantages and the most important ones include: (i) the CO tolerance of the Pt catalyst utilised in the electrode is very limited (tens of ppm) and (ii) a sluggish cathodic kinetic.

In order to overcome these drawbacks, it is advisable to increase the operational temperature to above 120 °C. Apart from this, high temperatures can provide other advantages and these are described in the literature [2–4]. An appropriate material for working under these conditions is polybenzimidazole (PBI). This material has certain advantages such as high proton conductivity when impregnated with a non-volatile acid (phosphoric acid), and exceptional thermal and chemical stability. These properties have driven the rapid development of PBI-based PEMFC systems since 1995, when it was first proposed by Savinell and co-workers [5].

PBI-based PEMFCs are composed by the classical PEMFC elements: electrolytic membrane (PBI), catalytic layer (Pt/C + PBI), gas diffusion layer (GDL; carbon substrate) and the monopolar/bipolar plates. It is evident that an optimum design, configuration and/or composition of all of these elements is fundamental in order to attain the highest and most stable possible cell performance. Thus, over the last 12 years there has been intensive research

activity devoted to the enhancement of this type of system. The properties of PBI membranes have been analysed with the aim of improving them and this research has been recently collected in the literature [3, 6, 7]. The most novel studies are mainly focused on the search for an appropriate catalyst that is capable of withstanding the stringent conditions under which H_3PO_4-doped-PBI-based PEMFC systems operate [8–11]. Nevertheless, in the field of GDLs, to the best of our knowledge only Seland et al. [12, 13] have referred to the effect of these materials.

The GDL in a fuel cell must fulfil several requirements [14–18]: (i) good diffusion properties in order to distribute the reactants evenly onto the electrode surfaces and to allow the exit of the water vapour (operational temperature is above 100 °C) produced at the cathode; (ii) low contact and bulk resistance to conduct electrons between the electrode and the flow field plate; (iii) physical durability to ensure gas tightness and adequate electrical contact. It is particularly important to consider criterion (i). In traditional low-temperature (Nafion®-based) PEMFC systems water is in the liquid state and it is crucial to manage this aspect to obtain good cell performance, especially at high current densities, in order to avoid electrode flooding problems. This limitation is expected to disappear above 100 °C as water is in the vapour state. However, it is important to have good diffusion properties to permit the exit of water vapour from the electrode to the plate channels. Nonetheless, it must born in mind that a high water vapour pressure due to an accumulation phenomenon would cause a reduction in the partial pressure of the reactants. This latter problem is only present in the cathode, provided that pre-humidification is not used in the system—a situation that is typical of PBI-based PEMFC systems. The GDL plays an important role in the improvement of the fuel cell performance, not only in terms of water flooding but also in terms of improving the access of the reactant gases (H_2, O_2 and air) and exit of the products (vapour) to/from the reactive layer (related to the permeation properties). The GDL also allows the transport of electronic charges between the flow fields and the catalytic layer. Different types of carbon supporting materials, thicknesses and Teflon (PTFE) loadings have been tested and marked differences have been observed in performance between them; i.e., by altering the GDL composition, fuel cell results can be significantly improved [14–45].

On the basis of the information discussed above, the goal of this work was to study the influence of the Teflon loading in the performance in a high temperature PEMFC. To achieve this aim, commercial Toray graphite carbon paper (wet-proofed with different Teflon loadings) was selected as the base support. The different GDLs were physically characterised by measuring the porosity (Hg-porosimetry), pore size distribution, SEM micrographs, hydrophobia level (*n*-decane/water method), air permeability (Darcy's law) and electrical resistance ("in-plane" and "through-plane"). Fuel cell measurements (with oxygen and air as comburent) were then carried out. Special attention had been paid to the mechanical properties of the GDLs, especially during their manufacturing and after their use in operation.

2 Experimental

2.1 Physical characterisation of the gas diffusion media

The following characterisation techniques were applied to commercial Toray Graphite Papers (TGPH-120) with Teflon contents of 0, 10, 20, and 40% (ETEK-Inc., USA, 0.35 mm thick).

Mercury porosimetry was used to determine the porosity of the samples. This also permitted the evaluation of the pore size distribution. The equipment used for the determination was a Micromeritics Auto Pore IV 9500 Hg porometer.

The surface morphologies of the different GDM samples were examined by scanning electron microscopy using a Philips XL30-CPDX4i microscope.

In order to assess the hydrophobia level of the sample, it was applied the *n*-decane/water method [16]. This method is fairly simple, and it consists of comparing the weight ratio differences when the sample was immersed in *n*-decane and in water. The expression for the calculation of this parameter is showed in Eq. 1.

$$\text{Hydrophobia level} = 1 - \frac{(m_{\text{water}} - m_{\text{dry}})}{(m_{n-\text{decane}} - m_{\text{dry}})} \quad (1)$$

where m_{water} (g), $m_{n\text{-decane}}$ (g) and m_{dry} (g) represent the sample weight after the immersion in water, *n*-decane and after drying in an oven for 1 h at 180 °C, respectively.

Another method widely applied for evaluating the hydrophobic properties of a GDM is the measurement of the contact angles between water and the carbon backings [14, 30]. For this, the sessile drop method was used, consisting of setting a droplet of water onto the surface (0.5 mL). The angle between the surface and the tangent in the contact point of the liquid/solid is measured. Large contact angles imply high hydrophobia.

Permeability was determined using Darcy's law [14, 16, 30, 32]. The permeability coefficient (k, m^2) can be calculated using the following expression:

$$k = \upsilon \cdot \mu \cdot \frac{1}{\Delta P} \quad (2)$$

where υ is the air flux (m s^{-1}), μ is the air viscosity (Pa s), l is the thickness of the sample (m), and ΔP is the pressure drop across the substrate (Pa).

Permeability was evaluated with apparatus designed and made in-house. In this set-up air flows through the GDM and the pressure drop is measured with a water column. Circular-shaped samples of 10 cm diameter were used for the measurements.

"In-plane" resistance was measured by a standard four point probe method [20, 22]. Impedance spectroscopy (EIS) was used to determine sample resistance using an Autolab PGSTAT30 Potentiostat/Galvanostat (Ecochemie, The Netherlands) equipped with a Frequency Response Analyser module. Sample resistivity was derived from the high frequency interception of the spectrum with the real axis and was calculated using Eq. 3. The great advantage of this method is that the values obtained correspond to pure bulk resistances.

$$\rho = R \cdot \frac{S}{l} \tag{3}$$

where ρ is the material resistivity (Ω cm), R is the resistance (Ω), S is the cross-section (cm^2) and l the thickness (cm).

"Through-plane" GDL resistivity was measured using apparatus designed and fabricated in-house. The set up consisted of two half "U" shape tubes between which the carbon paper was placed and securely clamped. The two tubes were then filled with mercury and contacts were made using copper wires. Voltage probes were located as close as possible to the GDL and current probes were located on the upper part of the tubes. Resistance was evaluated by impedance spectroscopy as described in the previous section.

The influence of the applied load on the total resistance was studied by sandwiching the MEA between two flat stainless steel plates. Two wires were welded to each plate, one for the current transient and the others as voltage probes. Squares of 3.3 × 3.3 cm^2 were used for the measurements. Ohm's law was directly applied for the calculation of the resistance. The total area resistance was obtained by multiplying the resistance by the section of the sample.

2.2 Fuel cell measurements

The preparation of a membrane-electrode-assembly (MEA) can be briefly described as follows. On top of each gas diffusion medium, the catalytic layer formed by 0.5 mg cm^{-2} of platinum from 20% Pt on Vulcan XC-72R carbon black (ETEK-Inc., USA) and 0.5 mg cm^{-2} PBI (from a 5% PBI solution in *N*,*N*′-dimethylacetamide) was deposited by an aerograph (N_2 as carrier gas). The gas diffusion electrodes were then cured in an oven for 2 h at 190 °C and soaked with a 10% wt. H_3PO_4 solution until a loading of 30 mg cm^{-2} was obtained on the electrodes, leaving them for at least 4 days in order to achieve complete impregnation. PBI membranes, produced according to the procedure described elsewhere [4], were immersed in an 80% H_3PO_4 bath (doping level of 6.7) and then removed and blotted with filter paper to remove the superficial acid. Hot-pressing to obtain the MEA was carried out by placing the membrane between the electrodes. A load of 1 ton (minimum applicable using our equipment) was subsequently applied at 130 °C for 15 min. A press for the preparation of IR pellets (Graseby Specac, United Kingdom) was modified and adapted for the membrane-electrode assembly process. The active area of the electrodes was 4.65 cm^2. Tests were carried out using the same GDLs in both anode and cathode, i.e., each MEA (pair of electrodes) had the same Teflon content, ranging from 0% to 40% (PTFE anode/cathode loadings: 0/0, 10/10, 20/20, and 40/40).

Measurements were taken using an Autolab PGSTAT 30 Potentiostat/Galvanostat equipped with a Current Booster (20 A). The cell was firstly conditioned at a fixed potential of 0.5 V and 125 °C for 24 h, with the system attaining a steady current after several hours, as reported elsewhere [11]. Once this period had elapsed, polarization curves were recorded in a potentio-dynamic polarization mode [38]. The potential was swept between the cell open circuit voltage and 0 V at 1 mV s^{-1}. The cell was always operated at 125 °C and atmospheric pressure. Hydrogen (99.999% pure, Praxair, Spain) was fed into the cell at a flow rate of 200 mL min^{-1}, whereas oxygen (99.999% pure, Praxair, Spain) was fed in at 40 mL min^{-1}. The oxygen was immediately replaced by air (99.999% pure, Praxair, Spain), keeping the same volumetric flow of oxygen, which entailed an air flow of 190 mL min^{-1}. Once again the cell was fixed at 0.5 V, even though measurements were now taken as soon as a stable current had been achieved. Subsequently, polarization curves with air were run. Cycles for the measurement of the polarization curves were repeated until reproducible ones were obtained.

3 Results and discussion

3.1 Porosity and pore size distribution

The porosity values are collected in Table 1. It has been reported that the bulk porosity directly influences the effective diffusion coefficient of a porous substrate [16]. Therefore, this parameter may affect the cell performance to some extent. On considering the values, it can be seen that there is a steady decrease in the porosity as the PTFE content increases. PTFE is impregnated on the untreated carbon substrate. This tends to accumulate at the fibre

Table 1 Values of the overall porosity, mean pore size, tortuosity and air permeability of the different PTFE-loaded carbon substrate

PTFE content (%)	Porosity from Hg-porosimetry (%)	Mean pore diameter (μm)	Tortuosity
0	76.3	39.4	2.932
10	73.9	36.7	3.363
20	69.6	33.9	3.582
40	61.6	31.6	4.377

crossing and, as a consequence, reduces the overall porosity.

The pore size distributions of the different PTFE-loaded carbon papers are represented in Fig. 1. The cumulative pore volume is shown in Fig. 1a and the specific pore volumes are given in Fig. 1b. According to Lee et al. [28] and Kong et al. [29], pore sizes can be classified into the following groups: (i) micropores, ranging from 0.03 to 0.06 μm; (ii) mesopores, ranging from 0.06 to 5 μm; and (iii) macropores, ranging from 5 to 20 μm. It can be seen in Fig. 1 that all the carbon substrates, regardless of the presence of PTFE, have a structure that is formed mainly by macropores, as over 90% of the pore volume resides in pores with a diameter larger than 5 μm, more specifically in the fraction between 20 and 70 μm (see Fig. 1c). Evidently, this leads to a mean pore size for the whole sample in the range 30–40 μm, as found by Mathias et al. [14] for Toray graphite papers. Nevertheless, it is noteworthy that these materials present a small fraction of pores in the limit between mesopores and macropores (5 μm) (Fig. 1d). This fraction decreases as the PTFE content is increased. As in the case of the macropres, PTFE will fill part of the mesoporous space. This, in turn, means that the mean pore size will decrease with the Teflon content, a situation that can be observed for all the samples. Tortuosity (τ) is another interesting parameter to be studied, as effective diffusion relies on it [$D_{\text{eff}} = (\varepsilon/\tau) \times D$] [16]. Tortuosity can be defined as the reciprocal of the ratio between the actual trajectory covered by the fluid when moving through the medium between two points and the rectilinear one. As expected, higher PTFE contents lead to greater tortuosity for any fluid when this penetrates into the GDL. Therefore, both the lower porosity and the higher tortuosity found on increasing PTFE loading have a negative impact on the diffusion of the reagent and product gases.

3.2 SEM micrographs

The surface morphologies of the four GDLs used in this work are shown in Fig. 2. On comparing these it can be seen that the higher the PTFE content, the less open the surface structure. As pointed out previously, Teflon deposits onto the carbon fibres and this reduces the overall porosity of the sample. This phenomenon is clearly reflected in the SEM micrographs. Furthermore, the sample with the highest PTFE content (40% PTFE) possesses a markedly "collapsed" structure, which could explain the

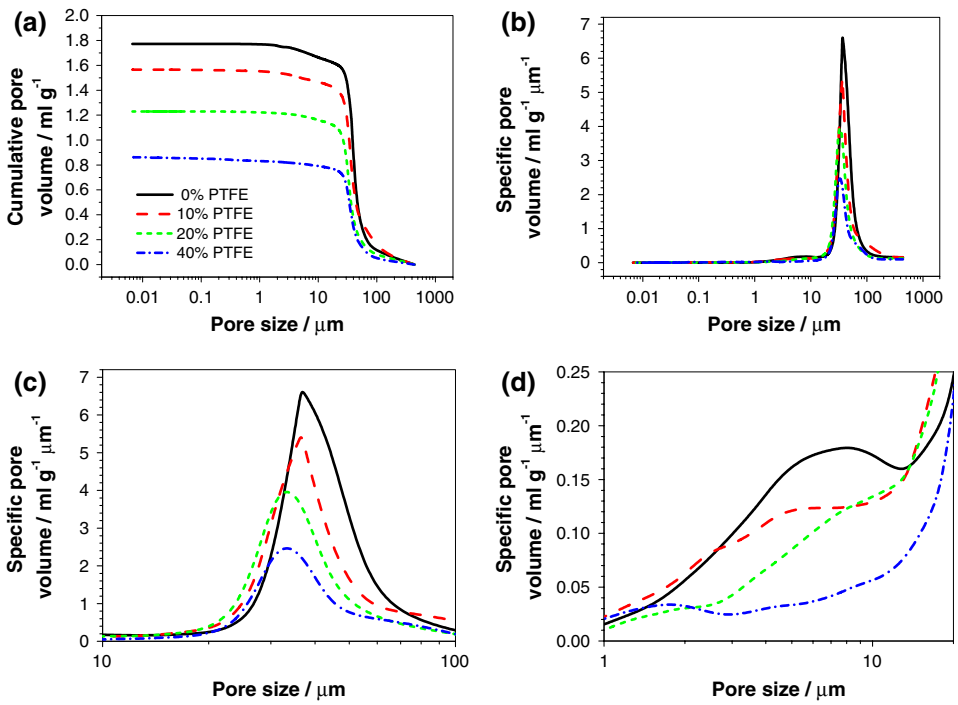

Fig. 1 (**a**) Cumulative and (**b–d**) specific pore size distribution of the different PTFE loaded carbon papers: (——) 0% PTFE; (— —) 10% PTFE; (- - - -) 20% PTFE; (— · —) 40% PTFE

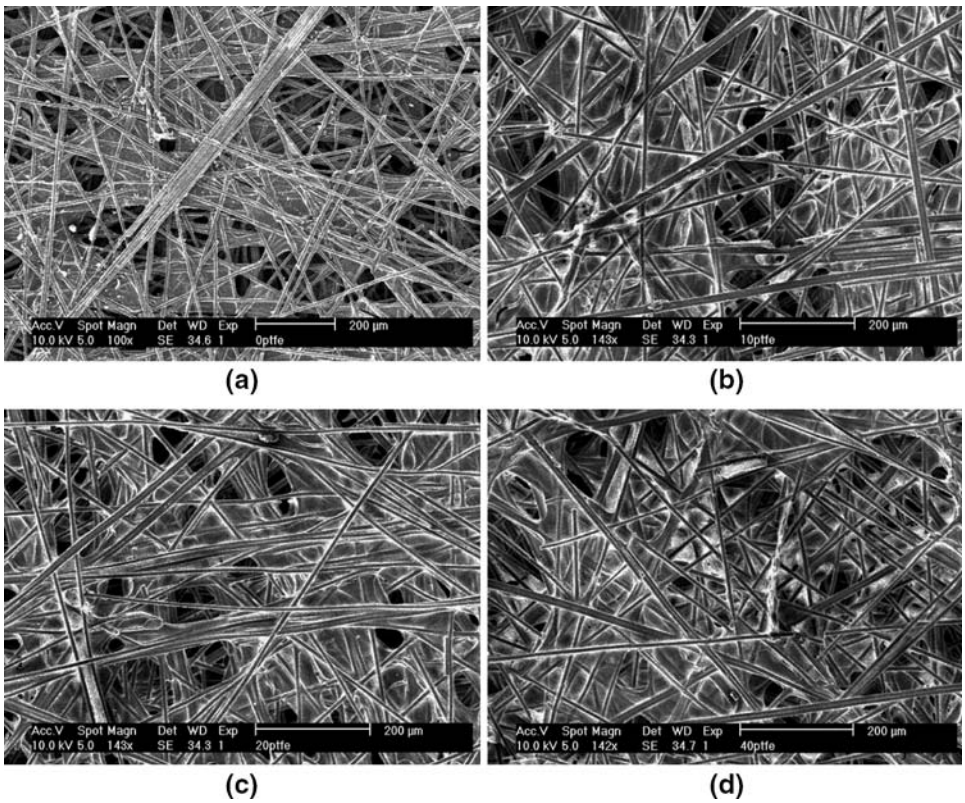

Fig. 2 SEM micrographs of the different PTFE loaded carbon papers: (**a**) 0% PTFE; (**b**) 10% PTFE; (**c**) 20% PTFE; (**d**) 40% PTFE

disappearance of the small pore fraction observed at 5 µm for the substrates with low Teflon loading.

3.3 Hydrophobicity

Table 2 collects the value of the hydrophobicity after applying Eq. 1. Hydrophobicity is already very high for the untreated carbon paper, as also showed Williams et al. [16]. Once the papers are wet-proofed, they almost become completely hydrophobic. More than 95% of the porous structure is formed by hydrophobic pores, where water cannot penetrate unless an over-hydraulic pressure is applied [18]. This shows the hydrophobic nature of carbon fibre supports despite not being wet-proofed.

Table 2 also collects the values of the corresponding left and right contact angles. All the angles are greater than 90°, indicating that the substrates are resistant to wetting, even when they have not been wet-proofed. When the paper is impregnated with PTFE, contact angles increase from $\approx$100° up to 155–160°. All the PTFE-loaded substrates display similar and high contact angles, and therefore, very high levels of hydrophobicity. It is also noteworthy that contact angles differ in the same sample depending upon the side. This seems to be due to the roughness of the sample surface. In any case, differences are small enough to be considered negligible.

3.4 Air permeability

The values of the air permeability for the different GDLs are shown in Table 2. The value obtained in this work for the carbon paper is in good agreement with other values reported in the literature, i.e. close to 10^{-11} m^2 [14, 16]. The trend is that the permeability diminishes as the PTFE content increases. The PTFE pore-blocking effect is responsible for the more difficult forced flow through the paper [19]. The larger fraction of pores, as expected and observed, enhances the gas permeability. This again indicates that higher Teflon content hinders the diffusion of the gases through the GDL and leads to lower mass transfer [14, 16, 30, 34, 42].

3.5 "In-plane" and "through-plane" electronic resistivity

The values of the "in-plane" and "through-plane" electronic resistivities of the samples are represented in Fig. 3a. It can be seen that, as one would expect, an increase in the PTFE content leads to increases in both material resistivities. Values obtained for the untreated carbon paper are similar to others reported in the literature [14, 16]. From this point of view, it is desirable to obtain a gas diffusion medium with the lowest possible electronic resistivity.

Table 2 Values of the hydrophobia level, left/right contact angles and air permeability of the different PTFE-loaded carbon substrate

PTFE content (%)	Hydrophobia level	Left contact angle (°)	Right contact angle (°)	10^{12} Air permeability (m^2)
0	80.3	100	95	9.21
10	97.3	158	160	7.77
20	98.5	155	151	6.36
40	99.5	155	160	3.46

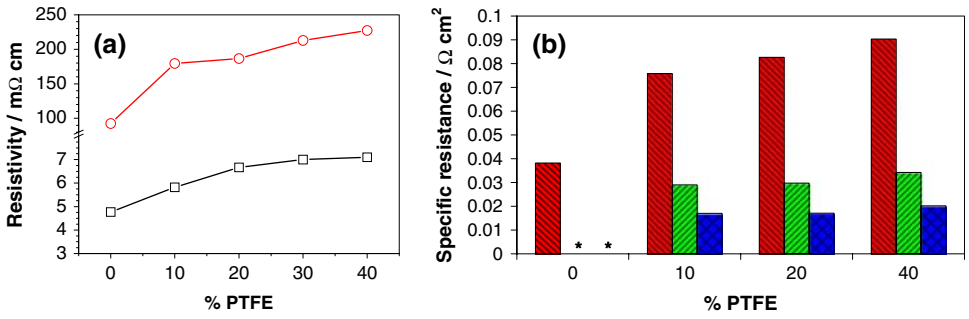

Fig. 3 (**a**) "In-plane" (□) and "through-plane" (○) electronic resistivity of the different PTFE loaded carbon papers; (**b**) Influence of the applied load on the "through-plane" total resistance for the different carbon substrate: (▨) 1 ton; (▨) 2 tons; (▨) 3 tons. (*Not measurable)

Hence, carbon paper that has not been wet-proofed seems to be the most appropriate material.

The "Mercury contacts" method is the most suitable way to minimise the contact resistance during the "through-plane" resistivity measurements. Unfortunately, contact resistance is present when operating a fuel cell [14, 46]. The effects of the applied pressure on the "through-plane" total resistance for all the PTFE-loaded carbon substrates are shown in Fig. 3b. An increase in pressure causes a decrease in the total resistance. This is due to the reduction in the contact resistance between the carbon paper and the stainless steel plates [34, 47, 48]. It is important to mention the fact that 0% PTFE carbon paper could be only measured when the minimum load was utilised. Higher loads caused partial disintegration of the carbon substrate. Therefore, in practical terms, a high assembly load should be applied to the fuel cell system in order to minimise the contact resistance and guarantee cell sealing. The upper limit of the applied load is defined by the physical integrity of the carbon support. Excessive loads detrimentally modify the properties in terms of electrical conduction and gas transport [49–51].

3.6 Fuel cell performance

The polarization curves for different pairs of electrodes with same Teflon loading in the GDL (0/0, 10/10, 20/20 and 40/40% PTFE) are shown in Fig. 4. Measurements were performed with oxygen as the comburent (Fig. 4a) and this was then changed to air (Fig. 4b).

In the case of oxygen, the performance levels at low current densities are fairly similar, indicating that the kinetics of the electrochemical reactions are not affected by the GDL. This trend was also observed by Yan et al. [43] and Chu et al. [44]. At medium current densities (linear region), increasing the PTFE content leads to slightly lower performance. The value of resistance, defined by the electrical resistance of the electrodes and by the resistance to the flow of ions in the electrolyte [52], can be calculated from the slope of the linear region—although this may also include linear diffusion terms due to diffusion of the gas phase in the diffusion layer [53]. Evidently, the higher the PTFE loading, the higher the ohmic term and the lower the porosity and permeability, both of which impair the mass transfer process. As a consequence, the additional contribution of a larger ohmic resistance and a more limited diffusion process explains the behaviour of the polarization curves at the intermediate current densities. At high current densities, where gaseous mass transportation dominates the cell performance, differences become more notable. The lower the Teflon content, the higher the ultimate current density, which again indicates that mass transfer processes occur more rapidly in GDLs with low PTFE loading. Using air (Fig. 4b) the results are significantly poorer due to the reduction in the oxygen partial pressure. As in the previous case, at low current density, the performances were similar for the four pairs of electrodes. At intermediate current densities, however, differences appear. On using air the mass transfer term becomes much more noticeable, which may explain the larger differences observed between the different GDL in the medium current density region compared to oxygen. At high current density the performance differences become much more marked. The best results are obtained for the non-Teflon-loaded GDL. As previously, the

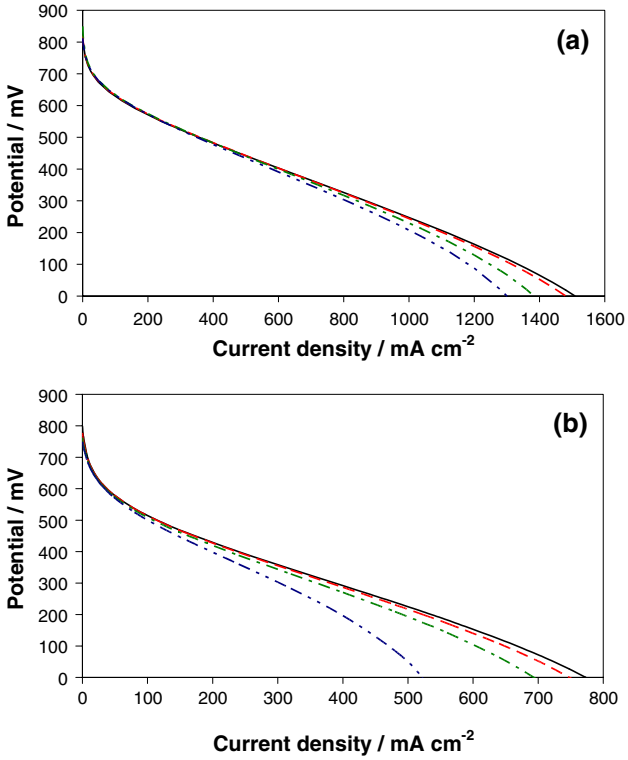

Fig. 4 Polarization curves for the different Teflon-loaded GDL: (——) 0% PTFE; (— —) 10% PTFE; (— · —) 20% PTFE; (— · · —) 40% PTFE. (**a**) With oxygen as comburent; (**b**) With air as comburent

lower the PTFE content, the higher the ultimate current densities that can be reached (773 mA cm^{-2} at 0 V for 0% PTFE, 748 mA cm^{-2} for 10% PTFE, 694 mA cm^{-2} for 20% PTFE and 522 mA cm^{-2} for 40% PTFE in the GDL). It is also clear that with air the differences at high current densities are larger than with oxygen. This can again be explained in terms of the lower O_2 availability.

Prasanna et al. [32, 34] and Yoon et al. [33] defined the oxygen gain as the difference between the cell voltage when oxygen is replaced by air as the oxidant for a given current density. Low oxygen gain means a rapid transport of oxygen through the electrode as a result of a less prominent blanketing effect of nitrogen in the oxidant. The oxygen gains of the previously described electrodes are shown in Fig. 5. It can be seen that higher PTFE contents lead to greater oxygen gain, especially in the region corresponding to high air current densities. Therefore, the nitrogen blanketing effect when oxygen is replaced by air is less noticeable for low (or zero) PTFE loadings. This means that oxygen is more easily transported along the GDL towards the catalyst sites and, therefore, mass transport limitations are smaller. Non-wet-proofed carbon paper seems to be the most appropriate for this system as it has the best oxygen transport properties.

In the above discussion it has been shown that the non-Teflon loaded GDL is the most suitable material as a gas

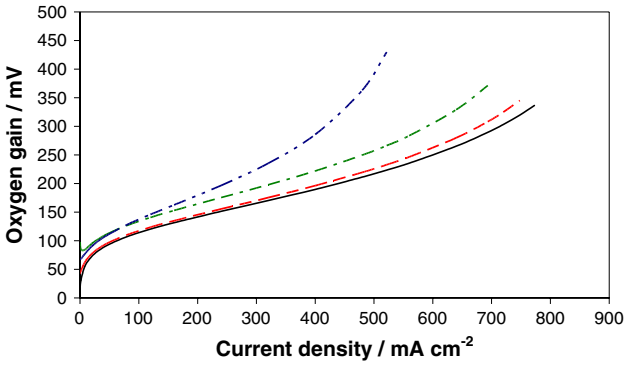

Fig. 5 Oxygen gain for the different Teflon-loaded GDL: (——) 0% PTFE; (— —) 10% PTFE; (— · —) 20% PTFE; (— · · —) 40% PTFE

diffusion medium (carbon fibres type) for PBI-based high temperature PEMFC systems. However, some practical problems were encountered with the non-Teflon-coated support in the procedure used here to prepare the MEA. After the hot pressing, some MEAs appeared damaged (more than 60% of the trials). Some parts of the carbon paper were almost broken or even partially disintegrated, showing that this material was not able to withstand the combination of high pressure and temperature used during the pressing. The detrimental effects that damage to the GDL have on the cell performance are shown in Figs. 6a, b for oxygen and air, respectively. The performance is notably lower for the partially destroyed MEA. The damage to the support could decrease the electrical conduction between it and the flow plate, thus decreasing the performance at medium current densities. In addition, the mass transfer characteristics of the GDL will be significantly modified, which is reflected in the polarization curves—particularly at high current densities—with a much better performance found for the MEA in good state. The lower O_2 partial pressure in air emphasizes the differences between the two MEAs. The oxygen gain is displayed in Fig. 6c. For comparison purposes, the results were normalized with respect to the maximum current densities obtained when the cell was run with oxygen (1,069 mA cm^{-2} for the damaged MEA and 1,509 mA cm^{-2} for the good one). Higher oxygen gains are obtained for the damaged MEA. Therefore, the damage in the carbon support has a negative effect on the transport of oxygen through it. The break-up of the layer seems to modify its porosity and permeability and, consequently, the gas transport is more difficult compared to that through the virgin support. This, for example, reflects on the value of the maximum oxygen gain and the ratio of the maximum current densities obtained for air and oxygen (see Fig. 6c). The maximum oxygen gain is higher for the damaged MEA, whereas the ratio of current densities is lower, reflecting again that oxygen transport is impeded to a

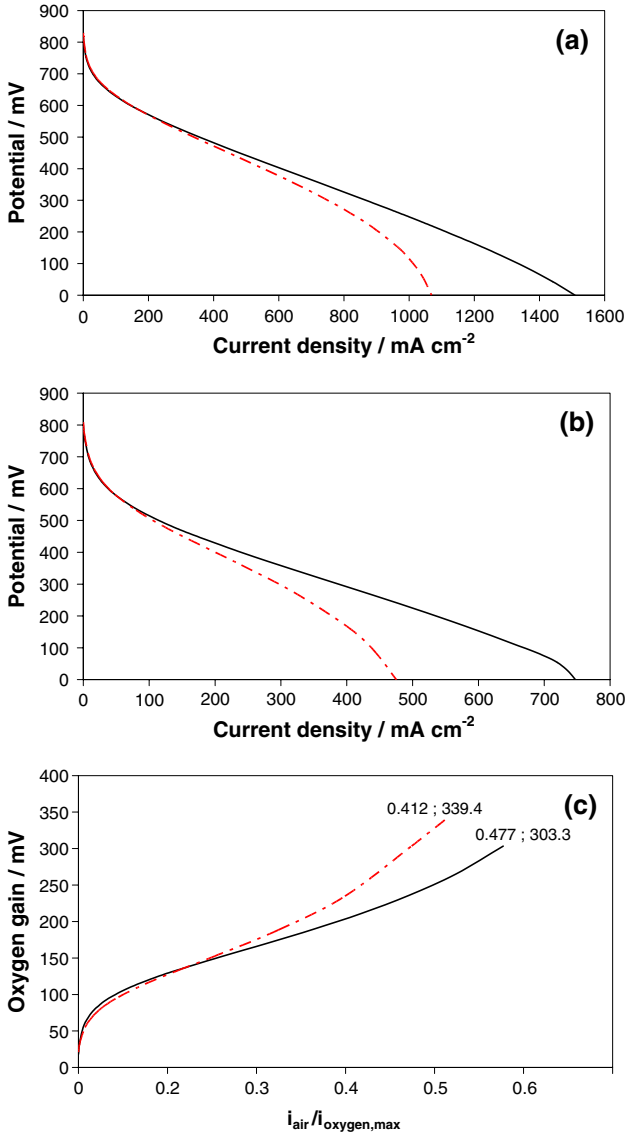

Fig. 6 Effects of damages of the GDL on the polarization curves for a non-Teflonized carbon paper loaded GDL: (——) good MEA; (— · —) damaged MEA (**a**) with oxygen as comburent; (**b**) with air as comburent; and (**c**) Relative oxygen gains (current was normalized respect to the maximum oxygen current density)

greater extent in the partially damaged MEA. It has also been reported [49–51] that when a carbon fibre support was damaged by the application of excessive loads, the cell performance dropped, in some cases abruptly. This phenomenon of breaking the GDL did not occur in the PTFE-loaded GDL and satisfactory MEAs were obtained from the press in all cases.

SEM micrographs (Fig. 2) help to understand the phenomenon described above. As can be seen in Fig. 2, untreated carbon paper is formed by graphite fibres that overlap one another and, in appearance, are joined very weakly compared to wet-proofed samples, where Teflon plays the role of a binder and consequently leads to an improvement in the GDL mechanical properties.

It is worth making a brief comparison between the results obtained for traditional low temperature Nafion®-based PEMFC. In these systems, the PTFE content greatly affects the cell performance. Low Teflon loadings improve the cell performance in terms of gas permeability, due to a more open porous structure and reduced electrical resistance. In terms of water flooding, in studies performed on carbon fibre papers, Park et al. [19] showed beneficial effects of low-loaded carbon papers over a wide range of relative humidity. However, Prasanna et al. [32] pointed out that PTFE contents below 20% promote mass transfer limitations due to inefficient water removal. In a study by Mathias et al. [14], non-wet-proofed carbon paper led to more problems with water management than teflonized paper. High PTFE-loaded carbon fibre papers limit the cell performance in terms of a large electrical resistance and reduced gas permeability. In addition, these materials appear to be very sensitive to humidity conditions. In general, these systems perform better under relatively dry conditions [14, 19, 38]. At high relative humidity they suffer from notable mass transfer limitations due to the high water retention capacity. As a consequence, carbon fibre supports seem to have an optimum PTFE content and this is in the low loading range (5–20%). For PEMFC systems operating above 100 °C, in principle, water flooding should not be a problem and it will not be considered in the discussion. Water ejection from the catalytic layer to the channels of the flow plates is considered to be driven by evaporation and, as a consequence, the results can be more easily explained. Low (or zero) PTFE-loaded GDL have higher gas permeabilities and reduced electrical resistances and they should therefore have a positive effect on the cell performance, facilitating the transient of the gases and the water vapour and the movement of electrical charge. High PTFE loadings lead to lower gas permeabilities and higher electrical resistance, which overall reduce the cell performance. This situation was demonstrated by the fuel cell results.

It is also interesting to compare these results with those obtained by the group of Tunold and co-workers [12, 13] as they also deal with a PBI-based PEMFC system. They found the addition of a certain amount of Teflon to be beneficial in preventing the paper from soaking during the spraying procedure and to reduce the penetration of carbon particles into the paper. They also reported that the bonding between the carbon support layer and the carbon paper was improved by wet-proofing. Although the method of preparation that they used for the electrodes was different in that they deposit a microporous layer before the catalytic one, whereas in this work the catalytic ink is directly sprayed onto the carbon paper, the results can be extrapolated, i.e., Teflon may also play a protective role for the catalytic layer as it does with

the microporous layer and also enhance the connection of this with the carbon paper. However, evidence for such behaviour was not observed. In the present work, the spraying procedure was carefully carried out in order to try to mitigate the soaking phenomenon, probably reducing the penetration of the catalyst particles into the carbon support. In fact, when there is a massive penetration of catalyst particles into the carbon support, a reduction in the catalytic activity is observed [23, 35, 39, 40] and this is reflected in the low current density behaviour of the cell [46, 52]. Similar behaviour was observed for the four cases studied, revealing analogous activity of the electrodes. The conditions for the spraying procedure were not described in detail in the publications by Tunold et al. and it is possible that variations in the spraying conditions might explain these differences. Finally, and according to the results, the quality of the connection between the carbon paper and the catalytic layer seems to be very similar regardless of the presence of Teflon. Once again, it is likely that the differences in the spraying conditions might explain the behaviour observed in this work compared to the results described by Tunold et al.

A summary of the findings drawn from the fuel cell results is shown in Fig. 7. The change in the ratio of the ultimate current density for air and oxygen and the maximum value of the oxygen gain versus the permeability for the different Teflon-loaded GDL are shown in Fig. 7a. The values of the slope of the linear region of the polarization curves for oxygen and air for the different Teflon loadings in the GDL are given in Fig. 7b. These figures again demonstrate that the results can be easily interpreted in terms of the reduced electrical resistance and enhanced mass transfer characteristics of the GDL as the PTFE content decreases. The combination of high porosity and permeability and low electrical resistance is the most suitable for fuel cells working above 100 °C. Thus, the non-teflonized carbon support can be proposed as an appropriate GDL, provided that its mechanical integrity can be maintained during the preparation and testing of the MEA. Otherwise, a certain amount of Teflon must be added to the untreated carbon to increase its mechanical resistance. When 10% PTFE carbon paper is used, the mechanical behaviour of the GDL is significantly enhanced, while good levels of electrical conduction and mass transfer characteristics are maintained in comparison to non-teflonized carbon paper. In fact, only a small performance drop was observed in the polarization curves (see Fig. 4a, b).

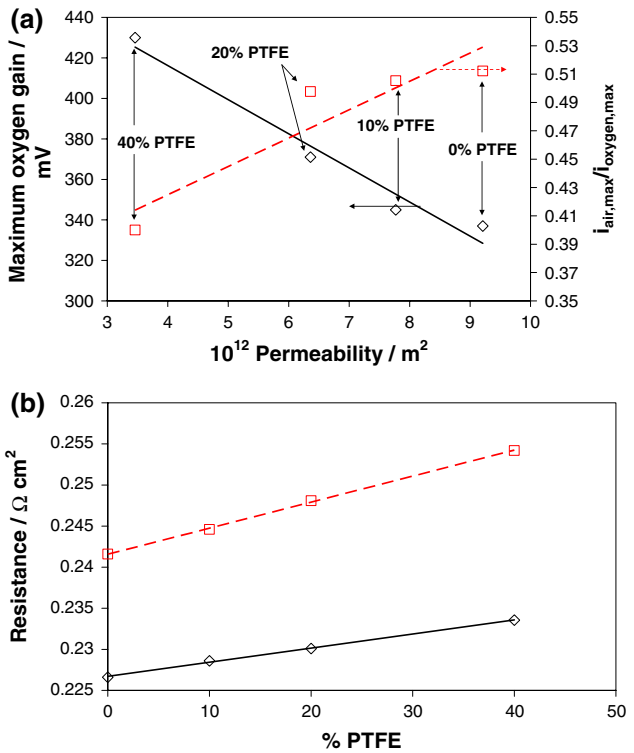

Fig. 7 (**a**) Maximum oxygen gain (◇) and ratio of ultimate current densities for air and oxygen (□) versus the permeability of the different Teflon-loaded GDL; (**b**) Slope of the linear region of the polarization curves for oxygen (◇) and air (□) for the different Teflon loadings in the GDL

4 Conclusions

A decrease in the porosity and permeability and an increase in the tortuosity, hydrophobicity, and electrical resistance were observed as the Teflon loading in the GDL was increased. This is significantly reflected in the fuel cell results. The lower the Teflon content, the better the cell performance. Hence, from the efficiency point of view, the use of a highly porous and permeable carbon paper with a low electrical resistance is advisable. However, the mechanical properties of the carbon in its use as GDL improve with the Teflon loading. Therefore, to obtain a good performance and, simultaneously, good mechanical properties of the GDLs, specially during their manufacturing and during their use in operation, the use of a minimally PTFE-loaded (10%) carbon paper is advisable because the inclusion of this level of Teflon improved properly the mechanical properties of the carbon support and only caused a very small drop in the performance.

Acknowledgements This work was funded by the Ministry of Education and Science of the Spanish Government through a project (CTM2004-03817), which includes a pre-doctoral grant awarded to J. J. Linares.

References

1. LaConti AB, Hamdan M, McDonald RC (2003) In: Vielstich W, Lamm A, Gasteiger HA (eds) Handbook of fuel cells, vol 3, chap 49. Wiley

2. Savadogo O (2004) J Power Sources 127:135
3. Li Q, He R, Jensen JO, Bjerrum NJ (2004) Fuel Cells 4:147
4. Lobato J, Cañizares P, Rodrigo MA, Linares JJ, Manjavacas G (2006) J Membr Sci 280:351
5. Wainright JS, Wang JT, Weng D, Savinell RF (1995) J Electrochem Soc 142:121
6. Wainright JS, Litt MH, Savinell RF (2003) In: Vielstich W, Lamm A, Gasteiger HA (eds) Handbook of fuel cells, vol. 3, chap 34, Wiley
7. Jones DJ, Rozière J (2001) J Membr Sci 185:41
8. Liu G, Zhang H, Zhai Y, Zhang Y, Xu D, Shao ZG (2007) Electrochem Commun 9:135
9. Zhai Y, Zhang H, Xing D, Shao ZG (2007) J Power Sources 164:126
10. Liu G, Zhang H, Zhong H, Hu J, Xu D, Shao Z (2006) Electrochim Acta 51:5710
11. Lobato J, Cañizares P, Rodrigo MA, Linares JJ (2007) Electrochim Acta 52:3910
12. Seland F, Berning T, Børresen B, Tunold R (2006) J Power Sources 160:27
13. Kongstein OE, Berning T, Børresen B, Seland F, Tunold R (2007) Energy 32:418
14. Mathias M, Roth J, Fleming J, Lehnert W (2003) In: Vielstich W, Lamm A, Gasteiger HA (eds) Handbook of fuel cells, vol 3, chap 46. Wiley
15. Ihonen J, Mikkola M, Lindbergh G (2004) J Electrochem Soc 151:1152
16. Williams MV, Begg E, Bonville L, Kunz HR, Fenton JM (2004) J Electrochem Soc 151:1173
17. Jordan LR, Shukla AK, Behrsing T, Avery NR, Muddle BC, Forsyth M (2000) J Power Sources 86:250
18. Benziger J, Nehlsen J, Blackwell D, Brennan T, Itescu J (2005) J Membr Sci 261:98
19. Park GG, Sohn YJ, Yang TH, Yoon YG, Lee WY, Kim CS (2004) J Power Sources 131:182
20. Antolini E, Pasos RR, Ticianelli EA (2002) J Appl Electrochem 32:383
21. Neergat M, Shukla AK (2002) J Power Sources 104:289
22. Passalacqua E, Squadrito G, Lufrano F, Patti A, Giorgi L (2001) J Appl Electrochem 31:449
23. Jordan LR, Shukla AK, Behrsing T, Avery NR, Muddle BC, Forsyth M (2000) J Appl Electrochem 30:641
24. Fischer A, Jindra J, Wendt H (1998) J Appl Electrochem 28:277
25. Antolini E, Pasos RR, Ticianelli EA (2002) J Power Sources 109:477
26. Giorgi L, Antolini E, Pozio A, Passalacqua E (1998) Electrochim Acta 43:3675
27. Zhao J, He X, Wang L, Tian J, Wan C, Jiang C (2007) Int J Hydrogen Energy 32:83
28. Lee HK, Park JH, Kim DY, Lee TH (2004) J Power Sources 131:200
29. Kong CS, Kim DY, Lee HK, Shul YG, Lee TH (2002) J Power Sources 108:185
30. Wang XL, Zhang HM, Zhang JL, Xu HF, Tian ZQ, Chen J, Zhong HX, Liang YM, Yi BL (2006) Electrochim Acta 51:4909
31. Shao ZG, Hsing IM, Zhang H, Yi B (2006) Int J Energy Res 30:1216
32. Prasanna M, Ha HY, Cho EA, Hong SA, Oh IH (2004) J Power Sources 131:147
33. Yoon YG, Park GG, Yang TH, Han JN, Lee WY, Kim CS (2003) Int J Hydrogen Energy 28:657
34. Prasanna M, Ha HY, Cho EA, Hong SA, Oh IH (2004) J Power Sources 137:1
35. Paganin VA, Ticcianelli EA, Gonzalez ER (1996) J Appl Electrochem 26:297
36. Lufrano F, Passalacqua E, Squadrito G, Patti A, Giorgi L (1999) J Appl Electrochem 29:445
37. Moreira J, Ocampo AL, Sebastián PJ, Smit MA, Salazar MD, del Angel P, Montoya JA, Pérez R, Martínez L (2003) Int J Hydrogen Energy 28:625
38. Lim C, Wang CY (2004) Electrochim Acta 49:4149
39. Song JM, Cha SY, Lee WM (2001) J Power Sources 94:78
40. Qi Z, Kaufman A (2002) J Power Sources 109:38
41. Chen J, Matsuura T, Hori M (2004) J Power Sources 131:155
42. Soler J, Hontañón E, Daza L (2003) J Power Sources 118:172
43. Yan WM, Soong CY, Chen F, Chu HS (2004) J Power Sources 125:27
44. Chu HS, Yeh C, Chen F (2003) J Power Sources 123:1
45. Jalani NH, Ramani M, Ohlsson K, Buelte S, Pacifico G, Pollard R, Staudt R, Datta R (2006) J Power Sources 160:1096
46. Fuel Cell Handbook, 7th edn. EG&G Technical Services, Inc., U.S. Department of Energy, November 2004
47. Wilde PM, Mändle M, Murata M, Berg N (2004) Fuel Cells 4:180
48. Escribano S, Blachot JF, Ethève J, Morin A, Mosdale R (2006) J Power Sources 156:8
49. Ge J, Higier A, Liu H (2006) J Power Sources 159:922
50. Lee WK, Ho CH, Van Zee JW, Murthy M (1999) J Power Sources 84:45
51. Lim C, Wang CY (2003) J Power Sources 113:145
52. Pan C, Li Q, Jensen JO, He R, Cleemann LN, Nilsson MS, Bjerrum NJ, Zeng Q (2007) J Power Sources 172:278
53. Antolini E, Passos RR, Ticianelli EA (2002) J Power Sources 109:477